# EVANS FUNCTIONS FOR INTEGRAL NEURAL FIELD EQUATIONS WITH HEAVISIDE FIRING RATE FUNCTION[*]

S COOMBES[†] AND M R OWEN[‡]

**Abstract.**

In this paper we show how to construct the Evans function for traveling wave solutions of integral neural field equations when the firing rate function is a Heaviside. This allows a discussion of wave stability and bifurcation as a function of system parameters, including the speed and strength of synaptic coupling and the speed of axonal signals. The theory is illustrated with the construction and stability analysis of front solutions to a scalar neural field model and a limiting case is shown to recover recent results of L. Zhang [On stability of traveling wave solutions in synaptically coupled neuronal networks, Differential and Integral Equations, 16, (2003), pp.513-536.]. Traveling fronts and pulses are considered in more general models possessing either a linear or piecewise constant recovery variable. We establish the stability of coexisting traveling fronts beyond a front bifurcation and consider parameter regimes that support two stable traveling fronts of different speed. Such fronts may be connected and depending on their relative speed the resulting region of activity can widen or contract. The conditions for the contracting case to lead to a pulse solution are established. The stability of pulses is obtained for a variety of examples, in each case confirming a previously conjectured stability result. Finally we show how this theory may be used to describe the dynamic instability of a standing pulse that arises in a model with slow recovery. Numerical simulations show that such an instability can lead to the shedding of a pair of traveling pulses.

**Key words.** traveling waves, neural networks, integral equations, Evans functions

**AMS subject classifications.** 92C20

**1. Introduction.** Traveling waves in neurobiology are receiving increased attention by experimentalists, in part due to their ability to visualize them with multi-electrode recordings and imaging methods. In particular it is possible to electrically stimulate slices of pharmacologically treated tissue taken from the cortex [19], hippocampus [27] and thalamus [25]. For cortical circuits such in vitro experiments have shown that, when stimulated appropriately, waves of excitation may occur [12, 36]. Such waves are a consequence of synaptic interactions and the intrinsic behavior of local neuronal circuitry. The propagation speed of these waves is of the order $\mathrm{cms}^{-1}$, an order of magnitude slower than that of action potential propagation along axons. The class of computational models that are believed to support synaptic waves differ radically from classic models of waves in excitable systems. Most importantly, synaptic interactions are non-local (in space), involve communication (space-dependent) delays (arising from the finite propagation velocity of an action potential) and distributed delays (arising from neurotransmitter release and dendritic processing). In many continuum models for the propagation of electrical activity in neural tissue it is assumed that the synaptic input current is a function of the pre-synaptic firing rate function [35]. These infinite dimensional dynamical systems typically take the form [15]

$$\frac{1}{\alpha}\frac{\partial u(x,t)}{\partial t} = -u(x,t) + \int_{-\infty}^{\infty} \mathrm{d}y\, w(y) f \circ u(x-y,t) - ga(x,t) \tag{1.1}$$

$$\frac{1}{\epsilon}\frac{\partial a(x,t)}{\partial t} = -a(x,t) + u(x,t). \tag{1.2}$$

Here, $u(x,t)$ is interpreted as a neural field representing the local activity of a population of neurons at position $x \in \mathbb{R}$, $f \circ u$ denotes the firing rate function and $w(y)$ the strength of connections between neurons

[†]Department of Mathematical Sciences, University of Nottingham, Nottingham, NG7 2RD, UK
[‡]Department of Mathematical Sciences, Loughborough University, Loughborough, Leicestershire, LE11 3TU, UK

separated by a distance $y$ (assuming a spatially homogeneous system). The constant $\alpha$ is the synaptic rate constant whilst the neural field $a(x,t)$ represents a local feedback signal, with strength $g > 0$, that modulates synaptic currents. Numerical simulations, with sigmoidal $f$, show that such systems support unattenuated traveling waves as a result of localized input. In the absence of a local feedback dynamics (i.e., $g = 0$), Ermentrout and McLeod [16] have established that there exists a unique monotone traveling front solution for sigmoidal firing rate functions and positive spatially decaying weight functions. Indeed, there are now a number of results about existence, uniqueness and asymptotic stability for integral differential equations, such as can be found in [2, 10, 11, 9]. Most recently Pinto and Ermentrout [30, 31] have constructed traveling pulse solutions using a singular perturbation argument for a general class of continuous firing rate functions. Moreover, for the special choice of a Heaviside firing rate function they have made extensive use of techniques pioneered by Amari [2] for the explicit construction of bumps and waves. For the case of standing pulses (and a more general form of local feedback than (1.2)) they have also given a rigorous analysis of the linearized equations of motion, allowing a discussion of bump stability. In this paper we extend this work to cover the stability of traveling (as well as standing) waves, using an Evans function approach. Moreover, we shall consider a general class of neural field theories that contains standard models, such as (1.1) and (1.2), as limiting cases.

The Evans function is a powerful tool for the stability analysis of nonlinear waves on unbounded domains. It has previously been used within the context of partial differential equations, but has also been recently formulated for neural field theories [37] and more general non-local problems [24]. The main use of the Evans function is in locating the point spectrum (isolated eigenvalues) of some relevant linearized operator. While its computation is typically only possible in perturbative situations, Zhang [37] has found an explicit formula for the Evans function for traveling waves of (1.1) and (1.2) with a Heaviside firing rate function. His approach makes explicit use of the inhomogeneous ordinary differential equation structure of the linearized equations of motion around a traveling wave. These are solved via the method of variation of parameters, with the source term arising from the non-local nature of the model. In this way he first constructs an intermediate Evans function for the homogeneous problem, before using this to determine the full Evans function in an appropriate right half plane. From here he is able to establish that the fast traveling pulse solution of the singly perturbed system (1.1) and (1.2), with $\epsilon \ll \alpha$ is exponentially stable. By working with integral rather than integro-differential models we shall develop three important extensions of this approach, side-stepping the need to construct an intermediate Evans function. These extensions cover i) the study of exponential wave stability in an integral framework rather than an integro-differential framework, which contains models like (1.1) and (1.2) as special cases, ii) avoiding the need to resort to the study of some singly perturbed system and iii) including the effects of space-dependent delays arising from axonal communication.

In section 2 we introduce the form of integral neural field model that we are concerned with in this paper. To solve the stability problem of the traveling wave solution, we rewrite the integral equations in moving coordinates and linearize about the traveling wave. Special solutions of this linearized system give rise to an eigenvalue problem and a linear operator $\mathcal{L}$. To establish the exponential stability of traveling wave solutions it suffices to investigate the spectrum of this operator. Since we are concerned with systems where the real part of the continuous spectrum has a uniformly negative upper bound, it is vitally important to determine the location of the isolated spectrum for wave stability. For the case of a Heaviside firing rate function we show in section 3 how this spectrum may be determined in terms of the zeros of a complex analytic function, which we identify as the Evans function. For illustrative purposes the focus of this section is on scalar integral models with traveling front solutions. In the next two sections we consider models with linear and nonlinear recovery variables respectively, that can also support traveling pulses. Throughout sections 3, 4 and 5 a number of examples are presented to illustrate the application of this theory. Moreover, we are able to establish a number of previously conjectured stability results. Finally in section 6 we discuss natural extensions of this work.

**2. Traveling waves.** In this section we introduce a more general integral form of equation (1.1) and consider the analysis of traveling wave solutions. For clarity we reserve discussion of feedback till later sections and take $g = 0$. Apart from a spatial integral mixing the network connectivity function with space-dependent delays, arising from non-instantaneous axonal communication, integral models can

naturally incorporate a temporal integration over some appropriately identified distributed delay kernel. These distributed delay kernels are biologically motivated and represent the response of (slow) biological synapses to spiking inputs. For a general firing rate function of synaptic current we consider the scalar integral equation:

$$u(x,t) = \int_{-\infty}^{\infty} \mathrm{d}y w(y) \int_0^{\infty} \mathrm{d}s \eta(s) f \circ u(x-y, t-s-|y|/v). \tag{2.1}$$

Here $v$ represents the velocity of action potential propagation [35, 22], whilst $\eta(t)$ ($\eta(t) = 0$ for $t < 0$) models the effects of synaptic processing. With the choice $\eta(t) = \alpha e^{-\alpha t}$ we recover the model given by (1.1). Some discussion of traveling wave solutions to (2.1) has previously been given in [13], where for some specific choices of $w(x)$ the equivalence to a certain partial differential equation (PDE) was exploited. Throughout this paper we shall avoid the use of such techniques and always work with integral equation models directly. However, again for simplicity, we shall consider the restriction $w(x) = w(|x|)$.

Following the standard approach for constructing traveling wave solutions to PDEs, such as reviewed by Sandstede [32], we introduce the coordinate $\xi = x - ct$ and seek functions $U(\xi, t) = u(x - ct, t)$ that satisfy (2.1). In the $(\xi, t)$ coordinates, the integral equation (2.1) reads

$$U(\xi, t) = \int_{-\infty}^{\infty} \mathrm{d}y w(y) \int_0^{\infty} \mathrm{d}s \eta(s) f \circ U(\xi - y + cs + c|y|/v, t - s - |y|/v). \tag{2.2}$$

The traveling wave is a stationary solution $U(\xi, t) = q(\xi)$ (independent of $t$), that satisfies

$$q(\xi) = \int_{-\infty}^{\infty} \mathrm{d}y w(y) \int_0^{\infty} \mathrm{d}s \eta(s) f \circ q(\xi - y + cs + c|y|/v). \tag{2.3}$$

The linearization of (2.2) about the steady state $q(\xi)$ is obtained by writing $U(\xi, t) = q(\xi) + u(\xi, t)$, and Taylor expanding, to obtain

$$u(\xi, t) = \int_{-\infty}^{\infty} \mathrm{d}y w(y) \int_0^{\infty} \mathrm{d}s \eta(s) f'(q(\xi - y + cs + c|y|/v))$$
$$\times u(\xi - y + cs + c|y|/v, t - s - |y|/v). \tag{2.4}$$

Of particular importance are bounded smooth solutions defined on $\mathbb{R}$, for each fixed $t$. Thus one looks for solutions of the form $u(\xi, t) = u(\xi)e^{\lambda t}$. This leads to the eigenvalue equation $u = \mathcal{L}u$:

$$u(\xi) = \int_{-\infty}^{\infty} \mathrm{d}y w(y) \int_{\xi-y+c|y|/v}^{\infty} \frac{\mathrm{d}s}{c} \eta(-\xi/c + y/c - |y|/v + s/c)$$
$$\times e^{-\lambda(-\xi/c + y/c + s/c)} f'(q(s))u(s). \tag{2.5}$$

Let $\sigma(\mathcal{L})$ be the spectrum of $\mathcal{L}$. We shall say that a traveling wave is linearly stable if

$$\max\{\mathrm{Re}(\lambda) : \lambda \in \sigma(\mathcal{L}), \ \lambda \neq 0\} \leq -K, \tag{2.6}$$

for some $K > 0$, and $\lambda = 0$ is a simple eigenvalue of $\mathcal{L}$. Furthermore, we shall take it that linear stability implies nonlinear stability.

In general the normal spectrum of the operator obtained by linearizing a system about its traveling wave solution may be associated with the zeros of a complex analytic function, the so-called Evans function. This was originally formulated by Evans [17] in the context of a stability theorem about excitable nerve axon equations of Hodgkin-Huxley type. Jones subsequently employed this function with some geometric techniques to establish the stability of fast traveling pulses in the FitzHugh-Nagumo model [23]. Following on from this, Alexander *et al.* formulated a more general method to define the Evans function for semi-linear parabolic systems [1]. Indeed this approach has proved quite versatile and has now been used to study the stability of traveling waves in a number of PDE models, such as discussed in [28, 4, 8, 32]. The extension to integral models is far more recent [37, 24]. However, it is fair to say,

that although there are many nonlinear evolution equations which support traveling wave solutions, there are very few which possess explicit Evans functions [29]. It is therefore all the more interesting that work by Zhang [37] on integral neural field models has shown that such explicit formulas are possible for the choice of a Heaviside firing rate function. This is one reason for us to pursue the choice of a Heaviside firing rate function. Another being that the qualitative features of traveling wave solutions for smooth sigmoidal firing rate functions, often used to describe biological firing rates, have previously been found to carry over to the case with a non-smooth Heaviside firing rate function [16, 30, 13]. Throughout the rest of this paper we shall therefore focus on the choice $f(u) = \Theta(u - h)$ for some threshold $h$. In this case the traveling wave is given by

$$q(\xi) = \int_0^\infty \eta(s)\psi(\xi + cs)\mathrm{d}s, \tag{2.7}$$

where

$$\psi(\xi) = \int_{-\infty}^\infty w(y)\Theta(q(\xi - y + c|y|/v) - h)\mathrm{d}y, \tag{2.8}$$

with $f'(q) = \delta(q - h)$. Note that this has a legitimate interpretation as $f'(q)$ only ever appears within an integral, such as (2.5). In the next section we will describe how to construct the Evans function for traveling wave solutions given by (2.7) and (2.8).

**3. Fronts in a scalar model.** In this section we introduce the techniques for constructing the Evans function with the example of traveling front solutions to (2.1). Previous work on the properties of such traveling fronts, i.e. speed as a function of system parameters, but not stability, can be found in [22, 30, 13]. Note also that a formal link between traveling front solutions in neural field theories and traveling spikes in integrate-and-fire networks can be found in [14]. We look for traveling front solutions such that $q(\xi) > h$ for $\xi < 0$ and $q(\xi) < h$ for $\xi > 0$. It is then a simple matter to show that

$$\psi(\xi) = \begin{cases} \int_{\xi/(1-c/v)}^\infty w(y)\mathrm{d}y & \xi \geq 0 \\ \int_{\xi/(1+c/v)}^\infty w(y)\mathrm{d}y & \xi < 0 \end{cases}. \tag{3.1}$$

The choice of origin, $q(0) = h$, gives an implicit equation for the speed of the wave as a function of system parameters.

The construction of the Evans function begins with an evaluation of (2.5). Under the change of variables $z = q(s)$ this equation may be written

$$u(\xi) = \int_{-\infty}^\infty \mathrm{d}y w(y) \int_{q(\xi-y+c|y|/v)}^{q(\infty)} \frac{\mathrm{d}z}{c} \eta(q^{-1}(z)/c - \xi/c + y/c - |y|/v)$$
$$\mathrm{e}^{-\lambda(q^{-1}(z)/c-\xi/c+y/c)} \times \frac{\delta(z - h)}{|q'(q^{-1}(z))|} u(q^{-1}(z)). \tag{3.2}$$

For the traveling front of choice we note that when $z = h$, $q^{-1}(h) = 0$ and (3.2) reduces to

$$u(\xi) = \frac{u(0)}{c|q'(0)|} \int_{-\infty}^\infty \mathrm{d}y w(y)\eta(-\xi/c + y/c - |y|/v)\mathrm{e}^{-\lambda(y-\xi)/c}. \tag{3.3}$$

From this equation we may generate a self-consistent equation for the value of the perturbation at $\xi = 0$, simply by setting $\xi = 0$ on the left hand side of (3.3). This self-consistent condition reads

$$u(0) = \frac{u(0)}{c|q'(0)|} \int_{-\infty}^\infty \mathrm{d}y w(y)\eta(y/c - |y|/v)\mathrm{e}^{-\lambda y/c}. \tag{3.4}$$

Importantly there are only non-trivial solution if $\mathcal{E}(\lambda) = 0$, where

$$\mathcal{E}(\lambda) = 1 - \frac{1}{c|q'(0)|} \int_{-\infty}^\infty \mathrm{d}y w(y)\eta(y/c - |y|/v)\mathrm{e}^{-\lambda y/c}. \tag{3.5}$$

From causality $\eta(t) = 0$ for $t \leq 0$ and physically $c < v$ so

$$\mathcal{E}(\lambda) = 1 - \frac{1}{c|q'(0)|} \int_0^\infty \mathrm{d}y w(y) \eta(y/c - y/v) \mathrm{e}^{-\lambda y/c}. \tag{3.6}$$

We identify (3.6) with the Evans function for the traveling front solution of (2.1). The Evans function is only real-valued if the eigenvalue parameter $\lambda$ is real. We see that the complex number $\lambda$ is an eigenvalue of the operator $\mathcal{L}$ if and only if $\mathcal{E}(\lambda) = 0$. Moreover, the algebraic multiplicity of an eigenvalue is exactly equal to the order of the zero of the Evans function.

From (2.7) and (2.8) it is also straight forward to calculate $q'(\xi)$ in the form

$$q'(\xi) = \int_{-\infty}^\infty \mathrm{d}y w(y) \int_0^\infty \mathrm{d}s \eta(s) \delta(q(\xi - y + cs + c|y|/v) - h) q'(\xi - y + cs + c|y|/v). \tag{3.7}$$

Proceeding as above for the construction of the Evans function it is simple to show that

$$q'(\xi) = u(\xi)|_{\lambda=0}, \tag{3.8}$$

where $u = \mathcal{L}u$. Thus $q'(\xi)$ is an eigenfunction of $\mathcal{L}$ for $\lambda = 0$ (expected from translation invariance). It is also a simple matter to check that $\mathcal{E}(0) = 0$, as expected. Introducing

$$\mathcal{H}(\lambda) = \int_0^\infty \mathrm{d}y w(y) \eta(y/c - y/v) \mathrm{e}^{-\lambda y/c}, \tag{3.9}$$

and using the fact that $\mathcal{E}(0) = 0$ allows us to write the Evans function in the form:

$$\mathcal{E}(\lambda) = 1 - \frac{\mathcal{H}(\lambda)}{\mathcal{H}(0)}. \tag{3.10}$$

To calculate the essential spectrum of the operator $\mathcal{L}$ we make use of the fact that $u(\xi)$ has the convolution form

$$u(\xi) = \frac{u(0)}{c|q'(0)|} \int_{-\infty}^\infty \mathrm{d}y w(y) \eta(y/c_\pm - \xi/c) \mathrm{e}^{-\lambda(y-\xi)/c}, \tag{3.11}$$

where $c_\pm^{-1} = c^{-1} \pm v^{-1}$ and we take $c_-$ when $\xi < 0$ and $c_+$ when $\xi > 0$. Introducing the Fourier transform

$$\widehat{u}(k) = \int_{-\infty}^\infty u(\xi) \mathrm{e}^{-ikx} \mathrm{d}\xi, \tag{3.12}$$

and taking the Fourier transform of (3.11), re-arranging and taking the inverse Fourier transform gives

$$\frac{|q'(0)|}{u(0)} \int_{-\infty}^\infty \mathrm{d}k \frac{\widehat{u}(k)}{\widehat{\eta}(-i\lambda - kc)} \mathrm{e}^{ik\xi} = \int_{-\infty}^\infty \mathrm{d}k \widehat{w} \left( \frac{kc}{c_\pm} \pm i\frac{\lambda}{v} \right) \mathrm{e}^{ik\xi}. \tag{3.13}$$

Assuming that $w(\xi)$ decays exponentially quickly then in the limit $|\xi| \to \infty$ the right-hand side of (3.13) vanishes (assuming $\mathrm{Re}\,\lambda < 0$). Seeking solutions of the form $u(\xi) = \mathrm{e}^{ip\xi}$, where $p \in \mathbb{R}$ gives

$$\frac{1}{\widehat{\eta}(-i\lambda - pc)} = 0. \tag{3.14}$$

This is an implicit equation for $\lambda = \lambda(p)$ that defines the essential spectrum of $\mathcal{L}$.

**3.1. Example: A traveling front.** Here we consider the choice $\eta(t) = \alpha e^{-\alpha t}$ and $w(x) = e^{-|x|}/2$ so that we recover a model previously analyzed by Zhang [37]. Assuming $c > 0$ the traveling front (2.7) is given in terms of (3.1) which takes the explicit form

$$\psi(\xi) = \begin{cases} \frac{1}{2}e^{m_- \xi} & \xi \geq 0 \\ 1 - \frac{1}{2}e^{m_+ \xi} & \xi < 0 \end{cases}, \qquad m_\pm = \frac{v}{c \pm v}. \tag{3.15}$$

The speed of the front is determined from the condition $q(0) = h$ as

$$c = \frac{v(2h - 1)}{2h - 1 - 2hv/\alpha}. \tag{3.16}$$

The essential spectrum is easily found using

$$\widehat{\eta}(k) = \frac{1}{1 + ik/\alpha}, \tag{3.17}$$

so that, from (3.14), $\lambda(p) = -\alpha + ipc$, i.e. a vertical line at Re $\lambda = -\alpha$. Hence, as stated earlier, the real part of the continuous spectrum has a uniformly negative upper bound and is not important for determining wave stability. The Evans function is easily calculated using the result

$$\mathcal{H}(\lambda) = \frac{\alpha}{2} \frac{1}{1 + \alpha \left( \frac{1}{c} - \frac{1}{v} \right) + \frac{\lambda}{c}}, \tag{3.18}$$

so that

$$\mathcal{E}(\lambda) = \frac{\lambda}{c + \alpha \left( 1 - \frac{c}{v} \right) + \lambda}. \tag{3.19}$$

The equation $\mathcal{E}(\lambda) = 0$ only has the solution $\lambda = 0$. We also have that

$$\mathcal{E}'(0) = \frac{1}{c + \alpha \left( 1 - \frac{c}{v} \right)} > 0, \tag{3.20}$$

showing that $\lambda = 0$ is a simple eigenvalue. Hence, the traveling wave front for this example is exponentially stable. Note that in the limit $v \to \infty$ we recover the result of Zhang [37]. We make the observation that axonal communication delays affect wave speed, but not wave stability.

**4. Traveling waves in a model with linear recovery.** In real cortical tissues there are an abundance of metabolic processes whose combined effect is to modulate neuronal response. It is convenient to think of these processes in terms of local feedback mechanisms that modulate synaptic currents. Such feedback may act to decrease activity in the wake of a traveling front so as to generate traveling pulses (rather than fronts). We will consider simple models of so-called *spike frequency adaptation* (i.e. the addition of a current that activates in the presence of high activity) that are known to lead to the generation of pulses for network connectivities that would otherwise only support traveling fronts [30]. Generalising the model in the previous section we write

$$Qu(x,t) = (w \otimes f \circ u)(x,t) - ga(x,t), \tag{4.1}$$
$$Q_a a(x,t) = u(x,t), \tag{4.2}$$

and we have introduced the notation

$$(w \otimes f)(x,t) = \int_{-\infty}^{\infty} w(y) f(x - y, t - |y|/v) \mathrm{d}y. \tag{4.3}$$

The (temporal) linear differential operators $Q$ and $Q_a$ have Green's functions $\eta(t)$ and $\eta_a(t)$ respectively so that

$$Q\eta(t) = \delta(t), \qquad Q_a \eta_a(t) = \delta(t). \tag{4.4}$$

This is a generalization of the model defined by (1.1) and (1.2). In its integrated form this more general model may be written

$$u = \eta * w \otimes f \circ u - g\eta_b * u, \tag{4.5}$$

where

$$(\eta * f)(x,t) = \int_0^t \eta(s)f(x,t-s)\mathrm{d}s, \tag{4.6}$$

and $\eta_b = \eta * \eta_a$. Proceeding as before we find that traveling wave solutions are given by

$$q(\xi) = \int_0^\infty \eta(s)\psi(\xi+cs)\mathrm{d}s - g\int_0^\infty \eta_b(s)q(\xi+cs)\mathrm{d}s, \tag{4.7}$$

with $\psi(\xi)$ given by (2.8). To obtain a solution for $q(\xi)$ it is convenient to take Fourier transforms and re-arrange to give

$$\widehat{q}(k) = \widehat{\eta}_c(k)\widehat{\psi}(k), \qquad \widehat{\eta}_c(k) = \frac{\widehat{\eta}(k)}{1 + g\widehat{\eta}_b(k)}, \tag{4.8}$$

where $\widehat{\eta}_b(k) = \widehat{\eta}(k)\widehat{\eta}_a(k)$. Equation (4.8) may then be inverted to give $q(\xi)$ in the explicit form

$$q(\xi) = \int_0^\infty \eta_c(z)\psi(\xi+cz)\mathrm{d}z, \tag{4.9}$$

where

$$\eta_c(t) = \frac{1}{2\pi}\int_{-\infty}^\infty \widehat{\eta}_c(k)\mathrm{e}^{ikt}\mathrm{d}k. \tag{4.10}$$

This last integral may be evaluated using a contour in the upper half complex plane for $t > 0$ (with $\eta_c(t) = 0$ for $t < 0$).

A traveling front solution is given by (4.9) and (3.1). The speed of the wave is again determined by the condition $q(0) = h$. Linearising around the traveling front and proceeding as before (for the case without recovery) we obtain an eigenvalue equation of the form $u = \mathcal{L}_c u$, where

$$\mathcal{L}_c u = \frac{u(0)}{c|q'(0)|}\int_{-\infty}^\infty \mathrm{d}y w(y)\eta_c(-\xi/c + y/c - |y|/v)\mathrm{e}^{-\lambda(y-\xi)/c}. \tag{4.11}$$

The essential spectrum $\lambda = \lambda(p)$ is determined from the solution of $1/\widehat{\eta}_c(-i\lambda - pc) = 0$. The Evans function of a front in this model with recovery is given by (3.10) with

$$\mathcal{H}(\lambda) = \int_0^\infty \mathrm{d}y w(y)\eta_c(y/c - y/v)\mathrm{e}^{-\lambda y/c}. \tag{4.12}$$

The model defined by (4.5) is also expected to support traveling pulses of the form $q(\xi) \geq h$ for $\xi \in [0,\Delta]$ and $q(\xi) < h$ otherwise. In this case the expression for $\psi(\xi)$ is given by

$$\psi(\xi) = \begin{cases} \mathcal{F}\left(\frac{-\xi}{1+c/v}, \frac{\Delta-\xi}{1+c/v}\right) & \xi \leq 0 \\ \mathcal{F}\left(0, \frac{\xi}{1-c/v}\right) + \mathcal{F}\left(0, \frac{\Delta-\xi}{1+c/v}\right) & 0 < \xi < \Delta \\ \mathcal{F}\left(\frac{\xi-\Delta}{1-c/v}, \frac{\xi}{1-c/v}\right) & \xi \geq \Delta \end{cases}, \tag{4.13}$$

where

$$\mathcal{F}(a,b) = \int_a^b w(y)\mathrm{d}y. \tag{4.14}$$

The dispersion relation $c = c(\Delta)$ is then implicitly defined by the simultaneous solution of $q(0) = h$ and $q(\Delta) = h$ ($\Delta > 0$). Linearising around the traveling pulse solution and proceeding as before we obtain an eigenvalue equation of the form $u = \mathcal{J}_c u$, where for $\xi \in [0, \Delta]$

$$\mathcal{J}_c u(\xi) = A_c(\xi, \lambda) u(0) + B_c(\xi, \lambda) u(\Delta). \tag{4.15}$$

Here the functions $A_c(\xi, \lambda)$ and $B_c(\xi, \lambda)$ are given by

$$A_c(\xi, \lambda) = \frac{1}{c|q'(0)|} \int_{\frac{\xi}{1-c/v}}^{\infty} \mathrm{d}y w(y) \eta_c(-\xi/c + y/c - y/v) \mathrm{e}^{-\lambda(y-\xi)/c} \tag{4.16}$$

$$B_c(\xi, \lambda) = \frac{1}{c|q'(\Delta)|} \int_{\frac{\xi-\Delta}{1+c/v}}^{\infty} \mathrm{d}y w(y) \eta_c((\Delta - \xi)/c + y/c - |y|/v) \mathrm{e}^{-\lambda(y-(\xi-\Delta))/c}. \tag{4.17}$$

Demanding that the eigenvalue problem $u = \mathcal{J}_c u$ be self-consistent at $\xi = 0$ and $\xi = \Delta$ gives the system of equations

$$\begin{bmatrix} u(0) \\ u(\Delta) \end{bmatrix} = \mathcal{A}_c(\lambda) \begin{bmatrix} u(0) \\ u(\Delta) \end{bmatrix}, \qquad \mathcal{A}_c(\lambda) = \begin{bmatrix} A_c(0, \lambda) & B_c(0, \lambda) \\ A_c(\Delta, \lambda) & B_c(\Delta, \lambda) \end{bmatrix}. \tag{4.18}$$

There is a nontrivial solution of (4.18) if $\mathcal{E}(\lambda) = 0$, where $\mathcal{E}(\lambda) = \det(\mathcal{A}_c(\lambda) - I)$. We recognize $\mathcal{E}(\lambda)$ as the Evans function for the traveling pulse solution.

Note that standing pulses are defined by $c = 0$ so that from (4.9)

$$q(\xi) = \widehat{\eta}_c(0) \int_0^{\Delta} w(\xi - y) \mathrm{d}y. \tag{4.19}$$

Hence, for a standing pulse

$$q'(\xi) = \widehat{\eta}_c(0)[w(\xi) - w(\xi - \Delta)], \tag{4.20}$$

and $|q'(0)| = |q'(\Delta)|$. Moreover, since $w(y)$ is relatively flat compared to $\eta_c(y/c)\mathrm{e}^{-\lambda y/c}/c$ when $c = 0$ the expressions for (4.16) and (4.17) simplify to

$$A_c(\xi, \lambda) = \frac{1}{|q'(0)|} \widehat{\eta}_c(-i\lambda) w(\xi) \mathrm{e}^{-\lambda \xi/v}, \qquad B_c(\xi, \lambda) = A_c(\Delta - \xi, \lambda). \tag{4.21}$$

In this case it can be shown that the Evans function $\mathcal{E}(\lambda)$ has zeros when

$$\frac{\widehat{\eta}_c(0)}{\widehat{\eta}_c(-i\lambda)} = \Gamma_{\pm}(\lambda), \tag{4.22}$$

where

$$\Gamma_{\pm}(\lambda) = \frac{w(0) \pm w(\Delta) \mathrm{e}^{-\lambda\Delta/v}}{|w(0) - w(\Delta)|}. \tag{4.23}$$

Note that $\lambda = 0$ is a solution as expected.

**4.1. Example: A front bifurcation.** Here we consider an example that recovers a model recently discussed by Bressloff and Folias [6] by choosing $\eta(t) = \alpha \mathrm{e}^{-\alpha t}$, $\eta_a(t) = \mathrm{e}^{-t}$ and $w(x) = \mathrm{e}^{-|x|}/2$. From (4.10) the function $\eta_c(t)$ is easily calculated given the pole structure of $\widehat{\eta}_c(k)$. Using the fact that $\widehat{\eta}(k) = (1 + ik/\alpha)^{-1}$ and $\widehat{\eta}_a(k) = (1 + ik)^{-1}$, this is given by

$$\widehat{\eta}_c(k) = \frac{-\alpha(1 + ik)}{(k - ik_+)(k - ik_-)}, \tag{4.24}$$

where

$$k_{\pm} = \frac{1 + \alpha \pm \sqrt{(1 + \alpha)^2 - 4\alpha(1 + g)}}{2}. \tag{4.25}$$

Hence, upon evaluating (4.10) using the calculus of residues we obtain

$$\eta_c(t) = \frac{\alpha}{k_- - k_+} \left\{ (1 - k_+)e^{-k_+ t} - (1 - k_-)e^{-k_- t} \right\}.$$ (4.26)

Using (4.9) and (3.15) the equation $q(0) = h$ gives an implicit expression for the front speed as

$$h = \frac{\alpha}{2} \frac{1 - cm_-}{(cm_-)^2 - cm_-(1+\alpha) + \alpha(1+g)} \qquad c > 0 \qquad (4.27)$$

$$h = -\frac{\alpha}{2} \frac{1 - cm_+}{(cm_+)^2 - cm_+(1+\alpha) + \alpha(1+g)} + \frac{1}{1+g} \qquad c < 0. \qquad (4.28)$$

Note that in the limit $v \to \infty$, $m_\pm \to \pm 1$ and we recover the result of Bressloff and Folias [6]. Re-arranging (4.27) and (4.28) gives $c$ in the form

$$cm_- = \frac{1}{2}\left[ 1 + \alpha - \frac{\alpha}{2h} \pm \sqrt{\left(1 + \alpha - \frac{\alpha}{2h}\right)^2 - 4\alpha\left(1 + g - \frac{1}{2h}\right)} \right] \qquad c > 0 \qquad (4.29)$$

$$cm_+ = \frac{1}{2}\left[ 1 + \alpha - \frac{\alpha}{2h^*} \pm \sqrt{\left(1 + \alpha - \frac{\alpha}{2h^*}\right)^2 - 4\alpha\left(1 + g - \frac{1}{2h^*}\right)} \right] \qquad c < 0, \qquad (4.30)$$

where $h^* = 1/(1+g) - h$. If $g = g_c$, where $2h(1+g_c) = 1$, there is a front for all $\alpha$ with speed $c = 0$. At a critical value of $\alpha$ this stationary front undergoes a pitchfork bifurcation leading to a pair of fronts traveling in opposite directions. If this critical condition is not met then the pitchfork bifurcation is broken as illustrated in figure 4.1. Since the zeros of $1/\hat{\eta}_c(k) = 0$ occur when $k = ik_\pm$ we see that the
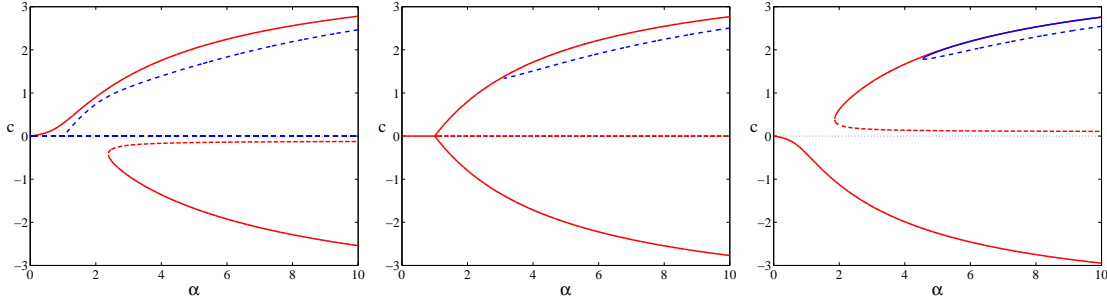


FIG. 4.1. *Wave front speed as a function of $\alpha$ for a model with linear recovery. If $g = g_c$, where $2h(1 + g_c) = 1$, there is a front for all $\alpha$ with speed $c = 0$. At a critical value of $\alpha$ this stationary front undergoes a pitchfork bifurcation leading to a pair of fronts traveling in opposite directions. This case is illustrated in the middle figure, where $v = 4$, $h = 0.25$ and $g = 1$. Away from this critical condition the pitchfork bifurcation is broken as illustrated in the left and right figures, where $g = 0.9$ and $g = 1.1$ respectively. Solid (dashed) lines are stable (unstable). The blue curves illustrate the existence of stable (solid) and unstable (dashed) pulses, whose speed and width are determined by the simultaneous solution of (4.33) and (4.34).*

essential spectrum is contained within the closed strip bounded by the two vertical lines $\lambda(p) = -k_\pm + ipc$. The Evans function may also be easily computed using

$$\mathcal{H}(\lambda) = \frac{\alpha}{2(k_- - k_+)}\left\{ \frac{1 - k_+}{1 + k_+(\frac{1}{c} - \frac{1}{v}) + \frac{\lambda}{c}} - \frac{1 - k_-}{1 + k_-(\frac{1}{c} - \frac{1}{v}) + \frac{\lambda}{c}} \right\}.$$ (4.31)

On the branch with $c = 0$ and $g = g_c$ (defining a stationary front) we find that

$$\mathcal{E}(\lambda) = \lambda \frac{(\lambda + k_+ + k_- - k_+ k_-)}{(\lambda + k_+)(\lambda + k_-)},$$ (4.32)

which has zeros when $\lambda = 0$ and $\lambda = k_+ k_- - (k_+ + k_-) = \alpha g_c - 1$. Hence, the stationary front changes from stable to unstable as $\alpha$ is increased through $1/g_c$. This result may also be used to infer the stability of the other branches in figure (4.1) (rather than laboriously evaluating the Evans function on each branch).

Examples of stationary fronts and fronts traveling in opposite directions, as predicted by the above analysis, are illustrated in figure 4.2. These simulations were implemented using the numerical scheme of Hutt *et al.* [21] to calculate the integral arising on the right hand side of (2.1). Fourier methods, as used previously by Coombes *et al.* [13], were found to give similar results. In figure 4.2, $g = 1.0, h = 0.25$ and $v = 4$, as in the second part of figure 4.1. The stationary front is stable for $\alpha = 0.9$, but for $\alpha > 1$ it loses stability in favor of a pair of moving fronts. As illustrated in figure 4.3, this symmetry breaking is reflected in the $u$-$a$ phase-plane. Here the stationary front lies on $a = u$, whilst the forward and backward fronts are distinguished by their trajectories on either side of $a = u$. Similar waves and bifurcations are found in a wide class of reaction-diffusion systems [20]. Note that initial conditions must be specified along with a history: the forward wave is generated by stimulating a previously inactive region, whereas the reverse wave is initiated by removing stimulation from a previously active region.
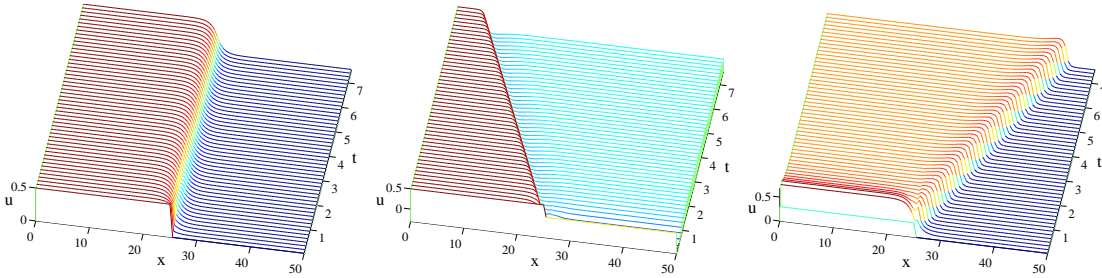


FIG. 4.2. *Illustrations of stationary, backward, and forward waves. In all cases, $g = 1.0$, $h = 0.25$, $v = 4$, corresponding to the second part of Figure 4.1. The stationary front has $\alpha = 0.9$, and the propagating waves have $\alpha = 10$.*
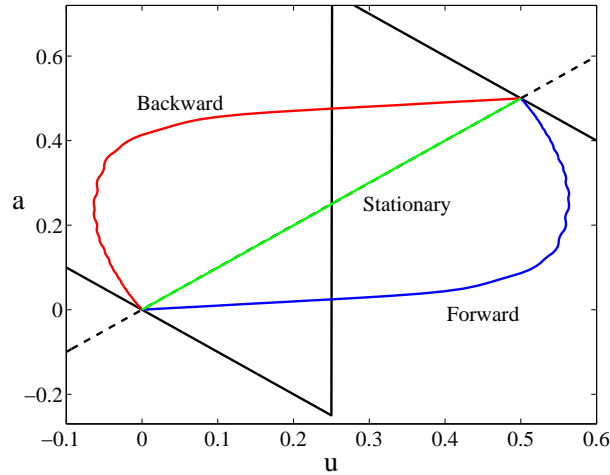


FIG. 4.3. *Phase planes corresponding to figure 4.1 and 4.2. The dashed black line denotes $a = u$, and the solid black line $a = (\Theta(u - h) - u)/g$. Forward and backward waves connect the same fixed points, but the different trajectories describe propagation in opposite directions.*

**4.1.1. Beyond the front bifurcation.** Motivated by results from the last example it is interesting to consider whether a stable traveling front and back with different speeds (that are stable in isolation) can interact to form new types of persistent solution. Numerical simulations show that if initially well separated front and back solutions are set up on a system then they will move apart if the relative speed of the two is positive and converge if it is negative. In the former case this leads to a widening region of activity, of the type shown in figure 4.4 (a). In the latter case the fronts can either annihilate or merge to form a traveling pulse, as illustrated in figures 4.4 (b) and 4.4 (c).

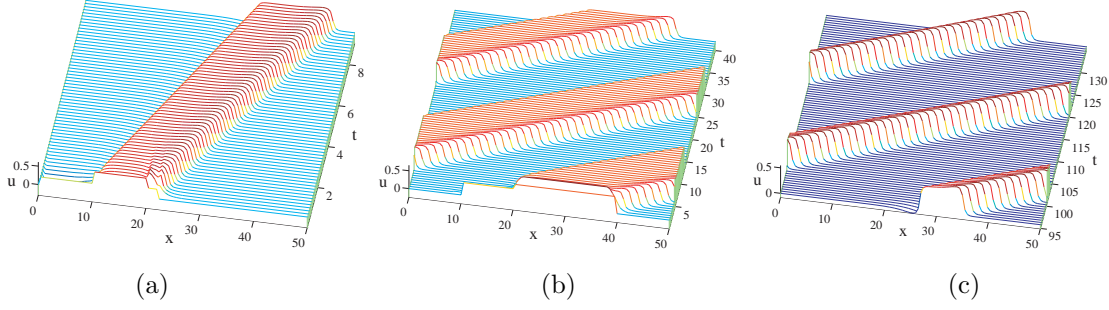The parameter regime that supports traveling pulses can be found by explicit construction. The

(a)  (b)  (c)

Fig. 4.4. *Interacting fronts either separate or converge. In the latter case a stable pulse may arise if parameters allow. (a) $g = 0.9$, (b,c) $g = 1.1$, the front moves more slowly than the back, and a pulse exists for these parameters ($v = 4, \alpha = 10, h = 0.25$). Part (b) shows the early evolution as the back begins to catch up with the front, and part (c) shows the final convergence to a pulse solution.*

existence of a pulse solution is determined by enforcing $q(0) = h = q(\Delta)$, giving:

$$h = \frac{\alpha(1 - e^{\Delta m_-})(1 - cm_-)}{2((cm_-)^2 - cm_-(1 + \alpha) + \alpha(1 + g))}, \tag{4.33}$$

$$h = \frac{1}{1 + g} + \alpha \frac{cm_- - 1}{2((cm_-)^2 - cm_-(1 + \alpha) + \alpha(1 + g))} - \alpha \frac{(1 - cm_+)e^{-\Delta m_+}}{2((cm_+)^2 - cm_+(1 + \alpha) + \alpha(1 + g))}$$

$$+ \frac{\alpha}{k_- - k_+} \left\{ (1 - k_-)e^{-\Delta k_-/c} \left( \frac{1}{k_-} + \frac{1}{2(cm_- - k_-)} + \frac{1}{2(cm_+ - k_-)} \right) \right.$$

$$\left. - (1 - k_+)e^{-\Delta k_+/c} \left( \frac{1}{k_+} + \frac{1}{2(cm_- - k_+)} + \frac{1}{2(cm_+ - k_+)} \right) \right\}. \tag{4.34}$$

Figure 4.5 shows the speed and width of such a traveling pulse as the conduction velocity $v$ varies. Note that pulses are not supported when the conduction velocity is too small, as there is a fold bifurcation with decreasing $v$. The speed of pulses as a function of $\alpha$ is also plotted in conjunction with that of fronts in figure 4.1, showing that stable pulses are preferred for $g > g_c$ and sufficiently large $\alpha$.
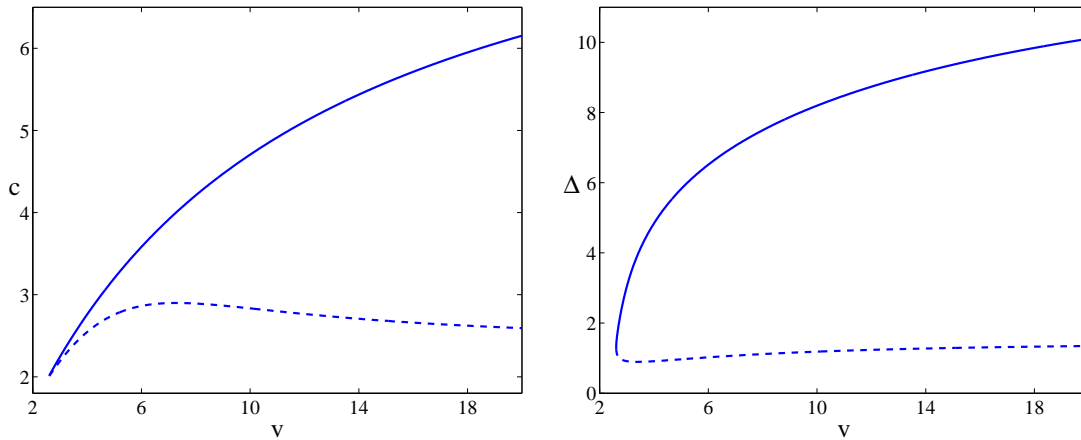


Fig. 4.5. *Speed and width of the traveling pulse as a function of $v$ in a neural model with linear recovery. The faster wave has the largest width. We note the fast and slow traveling pulse are annihilated in a saddle-node bifurcation with decreasing $v$. Here, $h = 0.25, \alpha = 1$ and $g = 1.1$. Solid (dashed) lines are stable (unstable).*

**4.2. Example: An unstable standing pulse.** In this example we consider the system discussed in section 4.1, but focus on standing pulses rather than traveling waves. For simplicity we shall also

consider the limit $v \to \infty$. From (4.13)

$$\psi(\xi) = \begin{cases} \frac{1}{2}(e^{\xi} - e^{\xi - \Delta}) & \xi \leq 0 \\ 1 - \frac{1}{2}(e^{\xi - \Delta} + e^{-\xi}) & 0 < \xi < \Delta \\ \frac{1}{2}(e^{-(\xi - \Delta)} - e^{-\xi}) & \xi \geq \Delta \end{cases} \tag{4.35}$$

and from (4.8) $\widehat{\eta}_c(0) = 1/(1+g)$. The pulse width is determined by setting $q(0) = h$ or equivalently $q(\Delta) = h$, to give

$$\Delta = -\ln[1 - 2h(1+g)], \qquad h \leq \frac{1}{2(1+g)}. \tag{4.36}$$

From (4.22) and (4.8) the zeros of the Evans function satisfy

$$\lambda^2 + \lambda[1 + \alpha - \alpha(1+g)\Gamma_{\pm}(0)] - \alpha(1+g)(\Gamma_{\pm}(0) - 1) = 0. \tag{4.37}$$

Since $\Gamma_-(0) = 1$ there are solutions of (4.37) with $\lambda = 0$ and $\lambda = \alpha g - 1$. The remaining solutions are given by

$$\lambda_{\pm} = \frac{-\Lambda \pm \sqrt{\Lambda + 4\alpha(1+g)(\Gamma_+(0) - 1)}}{2}, \tag{4.38}$$

with

$$\Lambda = 1 + \alpha - \alpha(1+g)\Gamma_+(0). \tag{4.39}$$

Since $\Gamma_+(0) > 1$ it follows that $\lambda_+ > 0$ and, hence, the stationary pulse is always unstable. In section 5 we shall consider a model with nonlinear recovery that can support a stable standing pulse.

**4.3. Example: A pair of traveling pulses.** Once again we consider the system discussed in section 4.2, but construct traveling rather than standing pulses. However, to recover a model discussed by Pinto and Ermentrout [30] we consider the case $Q_a = \partial_t$, or equivalently $\widehat{\eta}_a(k) = \lim_{\epsilon \to 0}(\epsilon + ik)^{-1}$. The function $\eta_c(t)$ is easily calculated as

$$\eta_c(t) = \frac{\alpha}{k_+ - k_-} \left\{ k_+ e^{-k_+ t} - k_- e^{-k_- t} \right\}, \tag{4.40}$$

with

$$k_{\pm} = \frac{\alpha \pm \sqrt{\alpha^2 - 4\alpha g}}{2}, \tag{4.41}$$

and $\psi(\xi)$ given by (4.35). It just remains to enforce the conditions $q(0) = h = q(\Delta)$, giving the two equations

$$h = \frac{\alpha c(1 - e^{-\Delta})}{2(c^2 + \alpha c + \alpha g)},$$

$$h = \frac{\alpha}{k_+ - k_-} \left\{ e^{-k_- \Delta/c} + \frac{k_-}{2} \left( \frac{e^{-\Delta} - e^{-k_- \Delta/c}}{k_- - c} + \frac{1 - e^{-k_- \Delta/c}}{k_- + c} \right) \right.$$

$$\left. - e^{-k_+ \Delta/c} - \frac{k_+}{2} \left( \frac{e^{-\Delta} - e^{-k_+ \Delta/c}}{k_+ - c} + \frac{1 - e^{-k_+ \Delta/c}}{k_+ + c} \right) \right\}. \tag{4.42}$$

We plot the simultaneous solution of these two equations in figure 4.6, showing the speed and width of the traveling pulse as a function of $g$. We note that there are two solution branches: one describing a fast wide pulse and the other a slower narrower pulse. Motivated by numerical experiments, Pinto and Ermentrout have conjectured that the larger (fast) pulse is stable and the narrower (slower) pulse unstable. We are now in a position to confirm this by examining the Evans function for a traveling pulse.
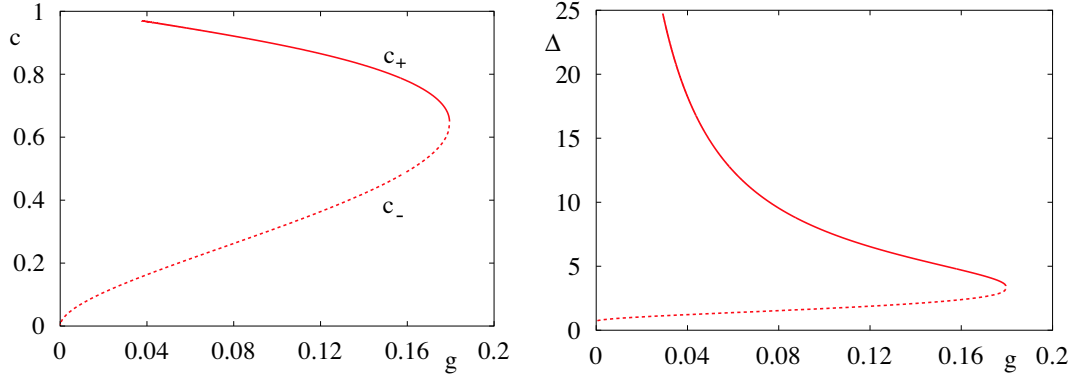
FIG. 4.6. *Speed and width of the traveling pulse as a function of g in a neural model with linear recovery. The faster wave, with speed $c_+$, has the largest width. We note the fast and slow traveling pulse are annihilated in a saddle-node bifurcation with increasing g, and that the width of the faster pulse diverges to infinity with decreasing g. Here, $h = 0.25$ and $\alpha = 1$. Solid (dashed) lines are stable (unstable).*

The functions $A_c(0,\lambda)$ and $B_c(0,\lambda)$ are calculated to be

$$A_c(0,\lambda) = \frac{1}{c|q'(0)|} \frac{\alpha}{k_+ - k_-} \frac{1}{2} \left\{ \frac{k_+}{1 + k_+/c + \lambda/c} - \frac{k_-}{1 + k_-/c + \lambda/c} \right\}, \tag{4.43}$$

$$B_c(0,\lambda) = \frac{1}{c|q'(\Delta)|} \frac{\alpha}{k_+ - k_-} \frac{1}{2} \left\{ k_+ \left( \frac{\mathrm{e}^{-(k_+ + \lambda)\Delta/c} - \mathrm{e}^{-\Delta}}{1 - k_+/c - \lambda/c} + \frac{\mathrm{e}^{-(k_+ + \lambda)\Delta/c}}{1 + k_+/c + \lambda/c} \right) \right.$$
$$\left. - k_- \left( \frac{\mathrm{e}^{-(k_- + \lambda)\Delta/c} - \mathrm{e}^{-\Delta}}{1 - k_-/c - \lambda/c} + \frac{\mathrm{e}^{-(k_- + \lambda)\Delta/c}}{1 + k_-/c + \lambda/c} \right) \right\}, \tag{4.44}$$

with $A_c(\Delta,\lambda) = \mathrm{e}^{-\Delta} A_c(0,\lambda)$, $B_c(\Delta,\lambda) = |q'(0)/q'(\Delta)| A_c(0,\lambda)$. Using the fact that for $v \to \infty$,

$$q'(\xi) = \int_0^\infty \eta_c(s)[w(\xi + cs) - w(\xi - \Delta + cs)]\mathrm{d}s, \tag{4.45}$$

we have that $q'(\Delta) = -h$ and

$$q'(0) = \frac{h}{1 - \mathrm{e}^{-\Delta}} - \frac{\alpha}{2(k_+ - k_-)} \left\{ \frac{k_+(\mathrm{e}^{-k_+\Delta/c} - \mathrm{e}^{-\Delta})}{c - k_+} - \frac{k_-(\mathrm{e}^{-k_-\Delta/c} - \mathrm{e}^{-\Delta})}{c - k_-} \right.$$
$$\left. + \frac{k_+\mathrm{e}^{-k_+\Delta/c}}{c + k_+} - \frac{k_-\mathrm{e}^{-k_-\Delta/c}}{c + k_-} \right\}. \tag{4.46}$$

The Evans function $\mathcal{E}(\lambda) = \det(\mathcal{A}_c(\lambda) - I)$ may then be calculated using (4.18). In figure 4.7 we show a section of the Evans function along the real axis for a wave on the fast branch and a wave on the slow branch. Also plotted is the Evans function for the wave that arises at the limit point in figure 4.6, where the fast and slow wave annihilate. This figure nicely illustrates that for a wave on the fast branch the Evans function has no zeros on the positive real axis, whilst the slow wave does. Moreover, as one moves around the branch from a fast to a slow wave the Evans function develops a repeated root at the origin, as expected. To further illustrate that the traveling pulse changes from stable to unstable as one moves around the limit point in figure 4.6 we track out the zero solution from figure 4.7 along the solution branch of figure 4.3, and plot this in figure 4.8.

**5. Pulses in a model of nonlinear recovery.** In this section we consider a system in which the recovery variable is governed by a nonlinear model, rather than a linear one as in section 4. Moreover, we shall consider the recovery process itself to be non-local and write

$$Qu(x,t) = (w \otimes f \circ u)(x,t) - g(w_a \otimes a)(x,t), \tag{5.1}$$
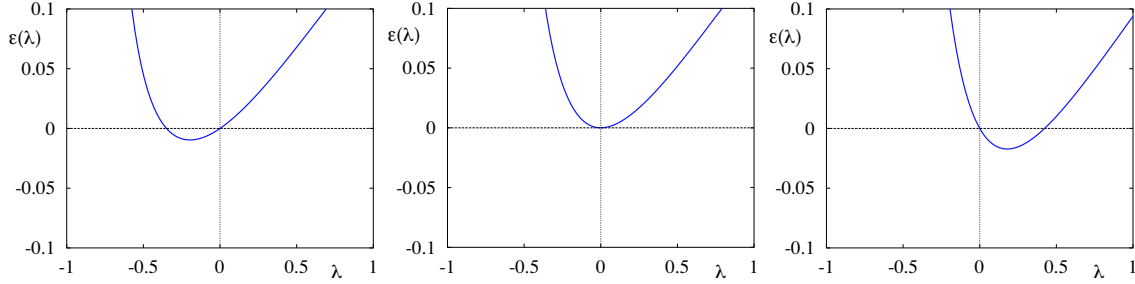$$Q_a a(x,t) = f \circ u(x,t). \tag{5.2}$$

FIG. 4.7. *A plot of $\mathcal{E}(\lambda)$ along the real axis for three different points on the solution branch shown in figure 4.6. In the figure on the left $g = 0.15$ with $c = c_+$ showing that a point on the fast branch has at least one zero on the negative real axis. Plotting over a much wider domain shows that there are no zeros on the positive real axis and that this graph asymptotes to 1. In the middle figure we see a repeated root at $\lambda = 0$ when $g = .1793$, corresponding to the limit point in figure 4.6 where a fast and slow wave merge. In the right hand figure $g = 0.15$ with $c = c_-$ and there is a zero of the Evans function on the positive real axis, showing that the slow branch is unstable. Note that $\lambda = 0$ is always a solution (as expected from translation invariance).*
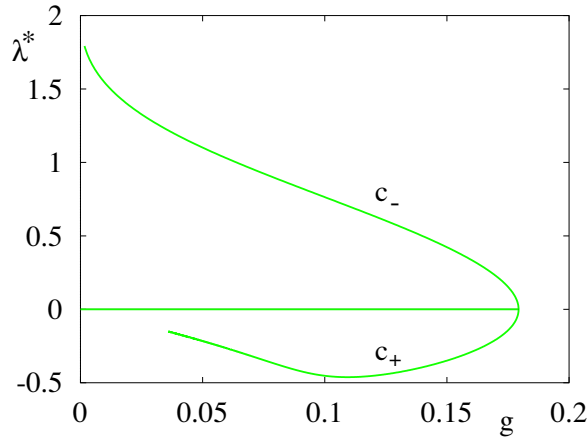


FIG. 4.8. *A plot of the zero of the Evans function, denoted $\lambda^*$, as seen in figure 4.7 along the solution branch seen in figure 4.6. Note that there is always a branch of solutions with $\lambda^* = 0$. The other branch passes through the origin where the slow and fast wave of figure 4.6 merge. We conclude that the fast wave ($c = c_+$) is stable and the slow wave ($c = c_-$) unstable.*

In keeping with earlier sections we consider the case when $w_a(x) = w_a(|x|)$. In its integrated form this model may be written

$$u = [\eta * w \otimes -g\eta_b * w_a \otimes] f \circ u. \tag{5.3}$$

This can be interpreted as a lateral inhibitory network model as in the paper of Pinto and Ermentout, or for the case with a relatively narrow footprint for $w_a(x)$ it may be regarded as a variant of the model with recovery described in section 4. In either case we shall show that the model can support stable standing pulses, unlike the case when the recovery variable evolves according to a linear model.

In a co-moving frame we have a modified form of (2.2) under the replacement $w(y)\eta(s) \to w(y)\eta(s) - gw_a(y)\eta_b(s)$. Hence, traveling wave solutions are given by

$$q(\xi) = \left( \int_{-\infty}^{\infty} dy\, w(y) \int_0^{\infty} ds\, \eta(s) - g \int_{-\infty}^{\infty} dy\, w_a(y) \int_0^{\infty} ds\, \eta_b(s) \right)$$
$$\times \Theta(q(\xi - y + cs + c|y|/v) - h). \tag{5.4}$$

Linearizing around a traveling pulse solution and proceeding as before we obtain an eigenvalue equation

of the form $u = \mathcal{L}u - g\mathcal{J}u$, where

$$\mathcal{J}u = \int_{-\infty}^{\infty} \mathrm{d}y w_a(y) \mathrm{e}^{-\lambda|y|/v} \int_0^{\infty} \mathrm{d}s \eta_b(s) \mathrm{e}^{-\lambda s} f'(q((\xi - y + cs + c|y|/v))$$
$$\times u(\xi - y + cs + c|y|/v), \tag{5.5}$$

and $\mathcal{L}$ is defined by (2.5). We may then proceed analogously as the case for the front solution described in section 3, for $\xi \in [0, \Delta]$, to obtain

$$\mathcal{L}u(\xi) = A(\xi, \lambda)u(0) + B(\xi, \lambda)u(\Delta), \qquad \mathcal{J}u(\xi) = C(\xi, \lambda)u(0) + D(\xi, \lambda)u(\Delta), \tag{5.6}$$

where

$$A(\xi, \lambda) = \frac{1}{c|q'(0)|} \int_{\frac{\xi}{1-c/v}}^{\infty} \mathrm{d}y w(y) \eta(-\xi/c + y/c - y/v) \mathrm{e}^{-\lambda(y-\xi)/c}, \tag{5.7}$$

$$B(\xi, \lambda) = \frac{1}{c|q'(\Delta)|} \int_{\frac{\xi-\Delta}{1+c/v}}^{\infty} \mathrm{d}y w(y) \eta((\Delta - \xi)/c + y/c - |y|/v) \mathrm{e}^{-\lambda(y-(\xi-\Delta))/c}, \tag{5.8}$$

$$C(\xi, \lambda) = \frac{1}{c|q'(0)|} \int_{\frac{\xi}{1-c/v}}^{\infty} \mathrm{d}y w_a(y) \eta_b(-\xi/c + y/c - y/v) \mathrm{e}^{-\lambda(y-\xi)/c}, \tag{5.9}$$

$$D(\xi, \lambda) = \frac{1}{c|q'(\Delta)|} \int_{\frac{\xi-\Delta}{1+c/v}}^{\infty} \mathrm{d}y w_a(y) \eta_b((\Delta - \xi)/c + y/c - |y|/v) \mathrm{e}^{-\lambda(y-(\xi-\Delta))/c}. \tag{5.10}$$

Demanding that perturbations be determined self consistently at $\xi = 0$ and $\xi = \Delta$ gives the system of equations

$$\begin{bmatrix} u(0) \\ u(\Delta) \end{bmatrix} = \mathcal{A}(\lambda) \begin{bmatrix} u(0) \\ u(\Delta) \end{bmatrix}, \qquad \mathcal{A}(\lambda) = \begin{bmatrix} A(0, \lambda) - gC(0, \lambda) & B(0, \lambda) - gD(0, \lambda) \\ A(\Delta, \lambda) - gC(\Delta, \lambda) & B(\Delta, \lambda) - gD(\Delta, \lambda) \end{bmatrix}. \tag{5.11}$$

There is a nontrivial solution of (5.11) if $\mathcal{E}(\lambda) = 0$, where $\mathcal{E}(\lambda) = \det(\mathcal{A}(\lambda) - I)$. We recognize $\mathcal{E}(\lambda)$ as the Evans function of a traveling pulse solution of (5.3). Working along identical lines to earlier sections the essential spectrum is defined by

$$\frac{1}{\widehat{\eta}(-i\lambda - pc)} \frac{1}{\widehat{\eta_a}(-i\lambda - pc)} = 0. \tag{5.12}$$

For standing pulses with $c = 0$, $Qu = u$ and $Q_a a = a$ so that

$$q(\xi) = \int_0^{\Delta} w_b(\xi - y) \mathrm{d}y, \tag{5.13}$$

where we have introduced the effective interaction kernel $w_b(x) = w(x) - gw_a(x)$. Hence,

$$q'(\xi) = w_b(\xi) - w_b(\xi - \Delta), \tag{5.14}$$

and we note that $|q'(0)| = |q'(\Delta)|$. For $c = 0$, $w(y)$ and $w_a(y)$ are relatively flat compared to $\eta(y/c)\mathrm{e}^{-\lambda y/c}/c$ and $\eta_b(y/c)\mathrm{e}^{-\lambda y/c}/c$ and we obtain the further simplification

$$A(\xi, \lambda) = \frac{1}{|q'(0)|} \widehat{\eta}(-i\lambda) w(\xi) \mathrm{e}^{-\lambda\xi/v}, \qquad\qquad B(\xi, \lambda) = A(\Delta - \xi, \lambda), \tag{5.15}$$

$$C(\xi, \lambda) = \frac{1}{|q'(0)|} \widehat{\eta_b}(-i\lambda) w_a(\xi) \mathrm{e}^{-\lambda\xi/v}, \qquad\qquad D(\xi, \lambda) = C(\Delta - \xi, \lambda). \tag{5.16}$$

**5.1. Example: A pair of traveling pulses.** Here we consider the choice $\eta(t) = \alpha e^{-\alpha t}$, $\eta_a(t) = e^{-t}$, $w(x) = e^{-|x|}/2$ and $w_a = \delta(x)$ so that we recover a model recently discussed by Coombes et al. [13]. With the use of the Evans function we will now establish the earlier conjecture of these authors that of the two possible co-existing traveling pulses in this model, it is the faster of the two that is stable. The traveling pulse solution for this model is given by [13]

$$q(\xi) = \frac{\alpha}{c} \int_\xi^\infty e^{\alpha(\xi - z)} [\psi(z) - ga(z)] dz, \tag{5.17}$$

where

$$a(\xi) = \begin{cases} [1 - e^{-\Delta/c}]e^{\xi/c} & \xi \le 0 \\ [1 - e^{(\xi-\Delta)/c}] & 0 < \xi < \Delta \\ 0 & \xi \ge \Delta \end{cases} \tag{5.18}$$

Using (4.13) $\psi(\xi)$ is given by

$$\psi(\xi) = \begin{cases} \frac{1}{2}(e^{m_+\xi} - e^{m_+(\xi-\Delta)}) & \xi \le 0 \\ 1 - \frac{1}{2}(e^{m_+(\xi-\Delta)} + e^{m_-\xi}) & 0 < \xi < \Delta \\ \frac{1}{2}(e^{m_-(\xi-\Delta)} - e^{m_-\xi}) & \xi \ge \Delta \end{cases} \tag{5.19}$$

In figure 5.1 we plot the speed of the pulse as a function of $g$, obtained by the simultaneous solution of $q(0) = h$ and $q(\Delta) = h$. This is reminiscent of that obtained for the model with linear recovery in section 4.3 (as also is the plot of $\Delta = \Delta(g)$, not shown). The essential spectrum for this problem is easily
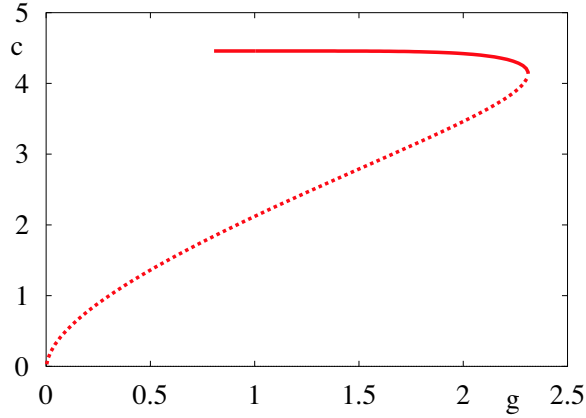


FIG. 5.1. *Speed of traveling pulse as a function of $g$ in a model with nonlinear recovery. Parameters are $h = 0.1$, $\alpha = 2$ and $v = 10$.*

calculated and can be shown to contain the closed strip bounded by the two vertical lines $\lambda = -\alpha + ipc$ and $\lambda = -1 + ipc$. It is also straightforward to obtain $C(0, \lambda) = C(\Delta, \lambda) = D(\Delta, \lambda) = 0$ and

$$A(0, \lambda) = \frac{1}{c|q'(0)|} \frac{\alpha}{2} \frac{1}{1 + \alpha\left(\frac{1}{c} - \frac{1}{v}\right) + \frac{\lambda}{c}}, \tag{5.20}$$

$$B(\Delta, \lambda) = \left|\frac{q'(0)}{q'(\Delta)}\right| A(0, \lambda), \tag{5.21}$$

$$A(\Delta, \lambda) = e^{-\Delta(v+\lambda)/(v-c)} A(0, \lambda), \tag{5.22}$$

$$B(0, \lambda) = \frac{1}{c|q'(\Delta)|} \frac{\alpha}{2} \left\{ \frac{e^{-(\alpha+\lambda)\Delta/c} - e^{-(v+\lambda)\Delta/(v+c)}}{1 - \alpha(\frac{1}{c} + \frac{1}{v}) - \frac{\lambda}{c}} + \frac{e^{-(\alpha+\lambda)\Delta/c}}{1 + \alpha\left(\frac{1}{c} - \frac{1}{v}\right) + \frac{\lambda}{c}} \right\}, \tag{5.23}$$

$$D(0, \lambda) = \frac{\alpha e^{-\Delta(1+\lambda)/c}}{c|q'(\Delta)|} \left(\frac{1 - e^{-\Delta(\alpha-1)/c}}{\alpha - 1}\right). \tag{5.24}$$

Moreover, we have simply that $-cq'(\phi) = -h + \psi(\phi) - ga(\phi)$ for $\phi \in \{0, \Delta\}$. One natural way to find the zeros of $\mathcal{E}(\lambda)$ is to write $\lambda = \nu + i\omega$ and plot the zero contours of Re $\mathcal{E}(\lambda)$ and Im $\mathcal{E}(\lambda)$ in the $(\nu, \omega)$ plane. The Evans function is zero where the lines intersect. We do precisely this in figure 5.2 for three distinct points on the solution branch shown in figure 5.1. On the fast branch it would appear that all the zeros of the Evans function lie in the left hand complex plane, whilst for the slow wave there is at least one in the right hand plane (on the real axis). As expected there is a double zero eigenvalue as one passes from the fast to the slow branch of traveling pulse solutions. Hence, the fast wave is stable and the slow wave unstable, confirming the numerical observations made in [13]. We note that in the presence
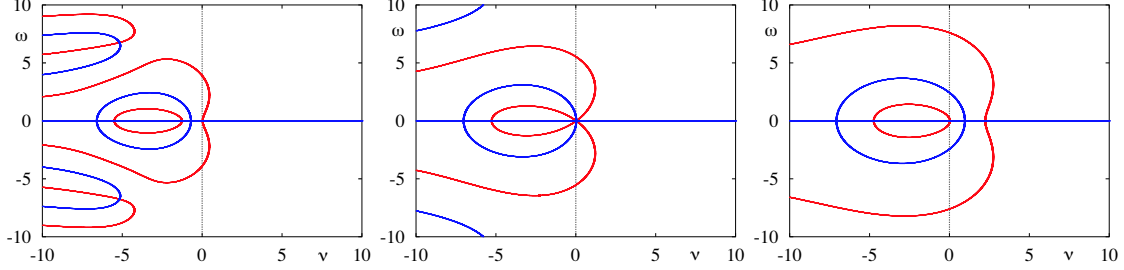


FIG. 5.2. *Evans function for a traveling pulse in a model with nonlinear recovery. Red lines indicate where Re $\mathcal{E}(\lambda) = 0$ and blue where Im $\mathcal{E}(\lambda) = 0$. Zeros of the Evans function occur at the intersection of red and blue lines. In the left hand figure $g = 2$ and a solution is taken from the fast branch. In the middle the value of $g$ is that at the saddle-node bifurcation from figure 5.1. On the right $g = 2$ with a solution taken from the slow branch. Other parameters are $h = 0.1$, $\alpha = 2$ and $v = 10$.*

of a discrete synaptic transmission delay, of duration $\tau_d$, we have the replacement $\eta(t) \rightarrow \eta(t - \tau_d)$. This causes the corresponding changes $A(\xi, \lambda) \rightarrow A(\xi + c\tau_d, \lambda)e^{-\lambda\tau_d}$, etc. and it is a simple matter to recalculate expressions (5.20) to (5.24). Although discrete delays influence the speed of solution, a direct examination of the Evans function in this case shows that they do not induce any new instabilities.

**5.2. Example: A dynamic instability of a standing pulse.** In this section we choose $\eta(t) = \alpha e^{-\alpha t}$, $\eta_a(t) = e^{-t}$, $w(x) = e^{-|x|}/2$ and $w_a(x) = e^{-|x|/\sigma_a}/(2\sigma_a)$ to recover a model of Pinto and Ermentrout [31]. In this case the standing pulse is given by

$$q(\xi) = \begin{cases} \frac{1}{2}(e^{\xi} - e^{\xi - \Delta}) - \frac{g}{2}(e^{\xi/\sigma_a} - e^{(\xi-\Delta)/\sigma_a}) & \xi \leq 0 \\ 1 - g - \frac{1}{2}(e^{\xi-\Delta} + e^{-\xi}) + \frac{g}{2}(e^{(\xi-\Delta)/\sigma_a} + e^{-\xi/\sigma_a}) & 0 < \xi < \Delta \\ \frac{1}{2}(e^{-(\xi-\Delta)} - e^{-\xi}) - \frac{g}{2}(e^{-(\xi-\Delta)/\sigma_a} - e^{-\xi/\sigma_a}) & \xi \geq \Delta \end{cases} . \tag{5.25}$$

Enforcing the condition $q(0) = h$ or $q(\Delta) = h$ generates the pulse width as a function of system parameters:

$$\frac{1}{2}(1 - e^{-\Delta}) - \frac{g}{2}(1 - e^{-\Delta/\sigma_a}) = h. \tag{5.26}$$

A plot of the pulse width as a function of the threshold parameter $h$ is shown in figure 5.3, showing that solutions come in pairs. We may then use (5.15) and (5.16) to construct the Evans function and plot it in the same fashion as the last example. However, unlike the last example we find that there is not a simple exchange of stability as one passes through the limit point defining the transition from a broad to a narrower pulse. Indeed we see from figure 5.4 that it is possible for a solution on the upper branch of figure 5.3 to undergo a *dynamic* instability with increasing $\alpha$. By dynamic we mean that a pair of complex eigenvalues crosses into the right hand plane on the imaginary axis, so that the standing pulse may begin to oscillate, as originally described in [31].

For the parameter values in figure 5.4 and choosing a value of $\alpha$ below that defining a dynamic instability, direct numerical simulations show that a bump solution is stable to random perturbations. In contrast, beyond the dynamic instability point, a bump solution can destabilize in favor of a homogeneous steady state. These two cases are illustrated in figure 5.5. The critical value of $\alpha$ defining a dynamic instability is found to depend only weakly on the value of the axonal conduction velocity $v$.
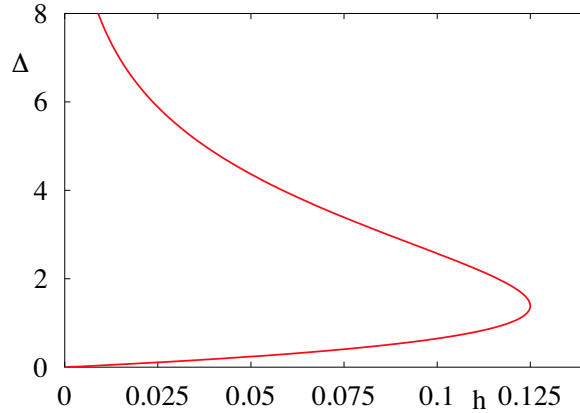
FIG. 5.3. *Pulse width as a function of threshold h in a model with lateral inhibition and nonlinear recovery. Here* $\sigma_a = 2$ *and* $g = 1$.
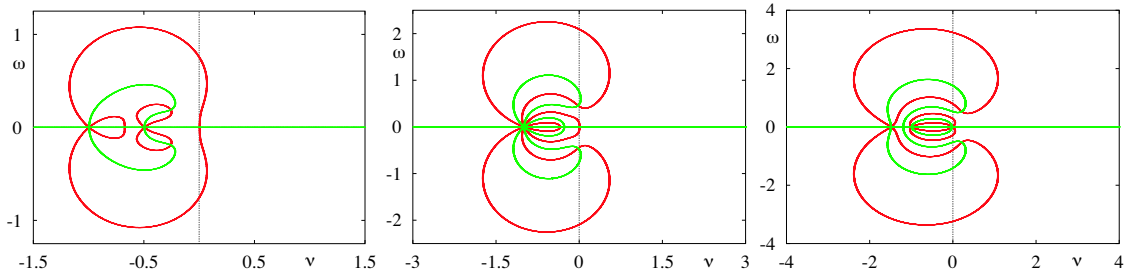


FIG. 5.4. *Evans function for the model with lateral inhibition and nonlinear recovery. Here* $h = 0.1$ *and* $v = 10$ *and a solution is taken from the branch with largest width* $\Delta$. *On the left* $\alpha = 0.5$, *and in the middle* $\alpha = 1.0$, *whilst on the right* $\alpha = 1.5$. *This illustrates the possibility of a dynamic instability with increasing* $\alpha$ *as a pair of complex eigenvalues crosses over to the right hand plane through the imaginary axis.*

For small values of the threshold $h$ the bump solution can develop a *dimple* such that $q'(0) > 0$. We plot the Evans function for a dimple solution in figure 5.6 and note that it also undergoes a dynamic instability with increasing $\alpha$. Interestingly, direct numerical simulations show that in this case the value of $v$ can have a more profound effect on the dynamics beyond the point of instability. For large values of $v$ an unstable solution collapses to a homogeneous steady state, whereas lower values of $v$ lead to the shedding of a pair of left and right traveling pulses. This is illustrated in figure 5.7.

**6. Discussion.** In this paper we have shown how to calculate the Evans function for integral neural field equations with a Heaviside firing rate function. Our work generalizes that of Zhang [37] on a certain integro-differential equation model in a number of ways. These include i) the study of exponential wave stability in an integral framework rather than an integro-differential framework ii) avoiding the need to resort to the study of some singly perturbed system and iii) including the effects of space-dependent delays arising from axonal communication. For the three main models that we have considered, i.e., a scalar integral neural field, a model with linear recovery and a model with nonlinear recovery, we have presented the explicit form for the Evans function for traveling fronts and pulses. Moreover, through a variety of examples we have shown that this is a powerful tool for the stability analysis of nonlinear waves and localized patterns in integral neural field models. In all cases the Evans function $\mathcal{E}(\lambda)$ is a complex analytic function of $\lambda \in \mathbb{C}$, with all the usual properties expected of such a function. Namely, $\mathcal{E}(\lambda) = 0$ if and only if $\lambda$ is an eigenvalue, the order of the roots is equal to the multiplicity of eigenvalues and for Re $\lambda > 0$, $\lim_{|\lambda| \to \infty} \mathcal{E}(\lambda) = 1$. This means that there is a positive constant $M$ such that $\mathcal{E}(\lambda) \neq 0$ for all $|\lambda| \geq M$. Since $\mathcal{E}(\lambda)$ is complex analytic there are at most finitely many eigenvalues within the disc $|\lambda| = M$. One could, of course, resort to the computation of $\mathcal{E}'(\lambda)/\mathcal{E}(\lambda)$ along the imaginary axis and
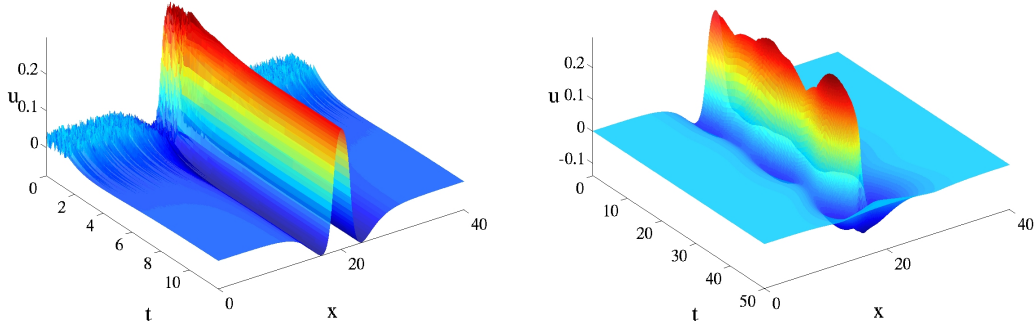
FIG. 5.5. *3-d plot of stable bump ($\alpha = 0.8$) and destabilized bump ($\alpha = 1.1$). $v = 1$, $h = 0.1$. The first has noisy initial data, with rapid convergence to the stable bump solution. The second case has initial data with $u(x, 0) = 1.05q(x)$ where $q(x)$ is the stationary bump solution.*
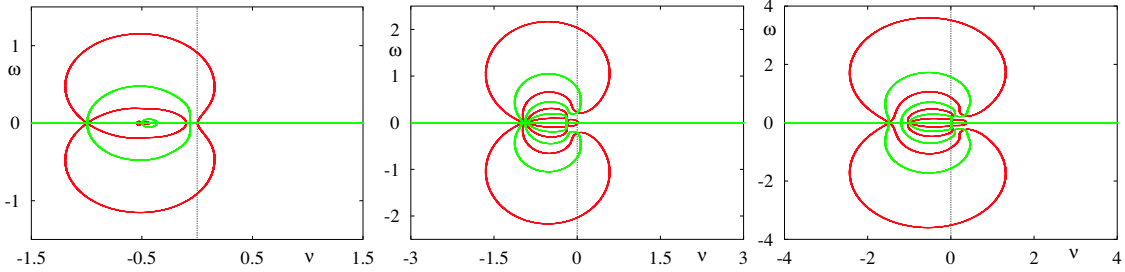


FIG. 5.6. *Evans function for the model with lateral inhibition and nonlinear recovery. Here $h = 0.025$ and $v = 1$ and a solution is taken from the branch with largest width $\Delta$. On the left $\alpha = 0.5$, and in the middle $\alpha = 0.9$, whilst on the right $\alpha = 1.5$. This illustrates the possibility of a dynamic instability with increasing $\alpha$ as a pair of complex eigenvalues crosses over to the right hand plane through the imaginary axis.*

use the argument principle to determine the number of zeros in the right half plane. Alternatively we could construct a Nyquist plot (the image of the Evans function along the imaginary axis) and count the number of times the graph winds around the origin. However, in this paper we have chosen simply to graphically find the intersection of the the zero contours of Re $\mathcal{E}(\lambda)$ and Im $\mathcal{E}(\lambda)$ in the complex plane.

There are a number of natural ways in which to extend the work presented in this paper. Perhaps the most natural extension is to consider the issue of a forced neural field where waves may lock to a moving stimulus. Another is to consider the use of averaging and homogenization theory to uncover the role of the periodic microstructure of cortex in front and pulse propagation and its failure, along the lines developed in [5, 7]. This is especially important when one recalls that the traveling front and pulse solutions considered in this paper are not structurally stable so that the introduction of even small inhomogeneities in the connectivity pattern may lead to propagation failure. Apart from recent work by Taylor [33], Werner and Richter [34], Laing and Troy [26] and Folias and Bressloff [18], planar studies have also received relatively little attention. Many of the techniques in this paper will carry over to the case of radially symmetric solutions, although the study of say, spiral stability, would first require the explicit construction of such solutions. However, the most obvious and major challenge is to extend this work to cover smooth sigmoidal firing rate functions. Even the numerical construction of the Evans function in this case is likely to be highly non-trivial, although there is some hope that recent Magnus methods developed by Aparicio *et al.* may be suited to this task [3]. These and other topics are ongoing areas of current research and will be reported on elsewhere.
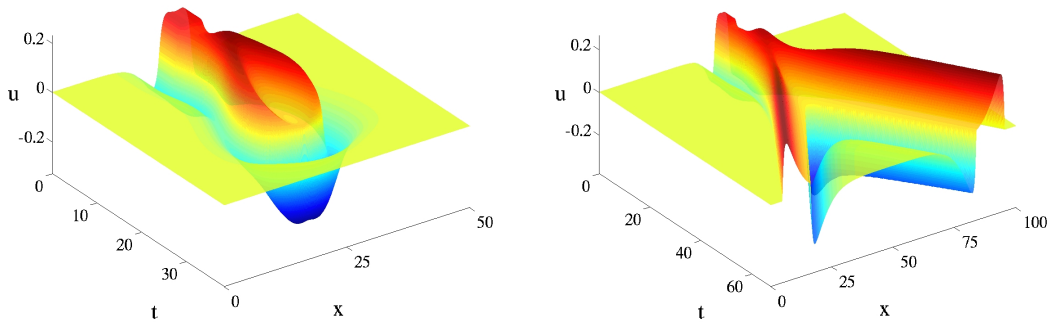
FIG. 5.7. $h = 0.025, \alpha = 1.1$, *the bump width is* 5.88. *Left:* $v = 8$, *the bump destabilizes and dies. Right:* $v = 1$, *as the bump dies, it sheds a pair of pulse waves.*

like to acknowledge the invitation from David Terman and Björn Sandstede to attend the workshop *Nonlinear integro-differential equations in Mathematics and Biology* March 3-5, 2003 at the Mathematical Biosciences Institute, Ohio State University, which directly motivated the work in this paper. SC would also like to acknowledge ongoing support from the EPSRC through the award of an Advanced Research Fellowship, Grant No. GR/R76219.

## REFERENCES

[1] J. Alexander, R. Gardner, and C. Jones, *A topological invariant arising in the stability analysis of travelling waves*, Journal für die reine und angewandte Mathematik, 410 (1990), pp. 167–212.

[2] S. Amari, *Dynamics of pattern formation in lateral-inhibition type neural fields*, Biological Cybernetics, 27 (1977), pp. 77–87.

[3] N. D. Aparicio, S. J. A. Malham, and M. Oliver, *Numerical evaluation of the Evans function by Magnus integration*, BIT, submitted (2004).

[4] N. J. Balmforth, R. V. Craster, and S. J. A. Malham, *Unsteady fronts in an autocatalytic system*, Proceedings of the Royal Society of London A, 455 (1999), pp. 1401–1433.

[5] P. C. Bressloff, *Traveling fronts and wave propagation failure in an inhomogeneous neural network*, Physica D, 155 (2001).

[6] P. C. Bressloff and S. E. Folias, *Front-bifurcations in an excitatory neural network*, SIAM Journal on Applied Mathematics, submitted (2004).

[7] P. C. Bressloff, S. E. Folias, A. Prat, and Y. X. Li, *Oscillatory waves in inhomogeneous neural media*, Physical Review Letters, 91 (2003), p. 178101.

[8] T. J. Bridges, G. Derks, and G. Gottwald, *Stability and instability of solitary waves of the fifth-order KdV equation: a numerical framework*, Physica D, 172 (2002), pp. 190–216.

[9] F. Chen, *Travelling waves for a neural network*, Electronic Journal of Differential Equations, 2003 (2003), pp. 1–4.

[10] X. Chen, *Existence, uniqueness, and asymptotic stability of traveling waves in nonlocal evolution equations*, Advances in Differential Equations, 2 (1997), pp. 125–160.

[11] Z. Chen, G. B. Ermentrout, and J. B. McLeod, *Traveling fronts for a class of nonlocal convolution differential equation*, Applicable Analysis, 64 (1997), pp. 235–253.

[12] R. D. Chervin, P. A. Pierce, and B. W. Connors, *Propagation of excitation in neural network models*, Journal of Neurophysiology, 60 (1988), pp. 1695–1713.

[13] S. Coombes, G. J. Lord, and M. R. Owen, *Waves and bumps in neuronal networks with axo-dendritic synaptic interactions*, Physica D, 178 (2003), pp. 219–241.

[14] D. Cremers and A. V. M. Herz, *Traveling waves of excitation in neural field models: equivalence of rate descriptions and integrate-and-fire dynamics*, Neural Computation, 14 (2002), pp. 1651–1667.

[15] G. B. Ermentrout, *Neural nets as spatio-temporal pattern forming systems*, Reports on Progress in Physics, 61 (1998), pp. 353–430.

[16] G. B. Ermentrout and J. B. McLeod, *Existence and uniqueness of travelling waves for a neural network*, Proceedings of the Royal Society of Edinburgh, 123A (1993), pp. 461–478.

[17] J. Evans, *Nerve axon equations: IV The stable and unstable impulse*, Indiana University Mathematics Journal, 24 (1975), pp. 1169–1190.

[18] S. E. Folias and P. C. Bressloff, *Breathing pulses in an excitatory neural network*, SIAM Journal on Applied Dynamical Systems, submitted (2004).

[19] D. GOLOMB AND Y. AMITAI, *Propagating neuronal discharges in neocortical slices: Computational and experimental study*, Journal of Neurophysiology, 78 (1997), pp. 1199–1211.

[20] A. HAGBERG AND E. MERON, *Pattern formation in non-gradient reaction-diffusion systems: the effects of front bifurcations*, Nonlinearity, 7 (1994), pp. 805–835.

[21] A. HUTT, M. BESTEHORN, AND T. WENNEKERS, *Pattern formation in intracortical neuronal fields*, Network, 14 (2003), pp. 351–368.

[22] M. A. P. IDIART AND L. F. ABBOTT, *Propagation of excitation in neural network models*, Network, 4 (1993), pp. 285–294.

[23] C. K. R. T. JONES, *Stability of the traveling wave solutions of the FitzHugh-Nagumo system*, Transactions of the American Mathematical Society, 286 (1984), pp. 431–469.

[24] T. KAPITULA, N. KUTZ, AND B. SANDSTEDE, *The Evans function for nonlocal equations*, Indiana University Mathematics Journal, to appear (2004).

[25] U. KIM, T. BAL, AND D. A. MCCORMICK, *Spindle waves are propagating synchronized oscillations in the ferret LGNd in vitro*, Journal of Neurophysiology, 74 (1995), pp. 1301–1323.

[26] C. R. LAING AND W. C. TROY, *PDE methods for nonlocal models*, SIAM Journal on Applied Dynamical Systems, 2 (2003), pp. 487–516.

[27] R. MILES, R. D. TRAUB, AND R. K. S. WONG, *Spread of synchronous firing in longitudinal slices from the CA3 region of Hippocampus*, Journal of Neurophysiology, 60 (1995), pp. 1481–1496.

[28] R. L. PEGO AND M. I. WEINSTEIN, *Eigenvalues, and instabilities of solitary waves*, Philosophical Transactions of the Royal Society London A, 340 (1992), pp. 47–94.

[29] ——, *Asymptotic stability of solitary waves*, Communications in Mathematical Physics, 164 (1994), pp. 305–349.

[30] D. J. PINTO AND G. B. ERMENTROUT, *Spatially structured activity in synaptically coupled neuronal networks: I. Travelling fronts and pulses*, SIAM Journal on Applied Mathematics, 62 (2001), pp. 206–225.

[31] ——, *Spatially structured activity in synaptically coupled neuronal networks: II. Lateral inhibition and standing pulses*, SIAM Journal on Applied Mathematics, 62 (2001), pp. 226–243.

[32] B. SANDSTEDE, *Handbook of Dynamical Systems II*, Elsevier, 2002, ch. Stability of travelling waves, pp. 983–1055.

[33] J. G. TAYLOR, *Neural 'bubble' dynamics in two dimensions: foundations*, Biological Cybernetics, 80 (1999), pp. 393–409.

[34] H. WERNER AND T. RICHTER, *Circular stationary solutions in two-dimensional neural fields*, Biological Cybernetics, 85 (2001), pp. 211–217.

[35] H. R. WILSON AND J. D. COWAN, *A mathematical theory of the functional dynamics of cortical and thalamic nervous tissue*, Kybernetik, 13 (1973), pp. 55–80.

[36] J.-Y. WU, L. GUAN, AND Y. TSAU, *Propagating activation during oscillations and evoked responses in neocortical slices*, Journal of Neuroscience, 19 (1999), pp. 5005–5015.

[37] L. ZHANG, *On stability of traveling wave solutions in synaptically coupled neuronal networks*, Differential and Integral Equations, 16 (2003), pp. 513–536.